now appeared in PCCP, 14, 5368 - 5375 (2012)

Temperature dependence of charge mobility in model discotic liquid crystals

Manuele Lamarra[†1], Luca Muccioli[*], Silvia Orlandi and Claudio Zannoni

Dipartimento di Chimica Fisica ed Inorganica and INSTM, Università di Bologna, IT-40136 Bologna, Italy

Email: Luca Muccioli*- Luca.Muccioli@unibo.it; Silvia Orlandi - S.Orlandi@unibo.it; Claudio Zannoni - Claudio.Zannoni@unibo.it;

*Corresponding author

[1]Deceased

Abstract

We address the calculation of charge carrier mobility of liquid-crystalline columnar semiconductors, a very promising class of materials in the field of organic electronics. We employ a simple coarse-grained theoretical approach and study in particular the temperature dependence of the mobility of the well-known triphenylene family of compounds, combining a molecular-level simulation for reproducing the structural changes and the Miller-Abrahams model for the evaluation of the transfer rates within the hopping regime. The effects of electric field, positional and energetic disorder are also considered. Simulations predict a low energetic disorder ($\simeq$ 0.05 eV), slightly decreasing with temperature within the crystal, columnar and isotropic phases, and fluctuations of the square transfer integral of the order of 0.003 eV^2. The shape of the temperature-dependent mobility curve is however dominated by the variation of the transfer integral and barely affected by the disorder. Overall, this model reproduces semi-quantitatively all the features of experimentally measured mobilities, on one hand reinforcing the correctness of the hopping transport picture and of its interplay with system morphology, and on the other suggesting future applications for off-lattice modeling of organic electronics devices.

1 Introduction

Discotic liquid crystals (DLCs) continue to attract considerable attention from the organic electronics community because of their semiconducting, self assembling and self healing properties, and their possible use as molecular wires. However their potential has not been fully exploited so far, mainly because of the competition with other materials such as organic crystals and polymers. Conjugated polymers are usually considered the most promising candidates for commercial devices because of their solution-processable nature, while small organic molecules are easier to synthesize and purify [1] and show superior charge mobilities in single crystals (> 10 cm^{2}V^{-1}s^{-1}). Columnar DLCs have, with respect to crystals, the ability of self heal and avoid grain boundaries, but generally show lower mobilities (< 1 cm^{2}V^{-1}s^{-1}). The mono-dimensional nature of charge transport in their columnar and crystal phases in fact results in a higher - and unwanted - sensitivity of the mobility to thermal fluctuations and structural defects [2,3]. In the theory of charge transport, these two effects are most often expressed in terms of the fluctuation of the electronic coupling between neighbouring molecules (the so-called off-diagonal or positional disorder) and of the energies of the molecules themselves (the diagonal or energetic disorder) [4]. The exploitation of DLCs in organic electronics devices requires then minimizing these two sources of disorder through improvements in chemical design, time and temperature stability, processing and aligning methods on surfaces. [5–9]

Optimization has as prerequisite the understanding of the microscopic origin of material and device behaviour. In this context, the combination of atomistic simulations to predict the morphology and of quantum mechanics (QM) for evaluating charge transport represents the state-of-the-art approach for investigating specific systems [2, 3, 10–12]. Recent studies carried out with this methodology underlined the validity the hopping picture of charge transport in DLCs [13] and the limiting effect of positional disorder on the mobility of the charge carriers in 1D systems [2,3]. In particular in references [3,11] it has been shown that for phthalocyanines and perylenes the calculated mobility drops of at least of one order of magnitude if a time-independent positional disorder is included.

The main drawback of atomistic modeling is its computational cost, which severely limits the system size and the time span of the investigation [14] and makes this type of calculations not affordable for simulating an operating device. As a consequence, device modeling often resorts to rather crude approximations for the morphology of the system, usually described as a cubic lattice of sites, where each site represents a nanometric size domain of the semiconducting material. While this level of description can be appropriate to amorphous polymers [15–20], it could be judged too rough for molecular crystals or liquid crystals because it neglects the molecular shape, the intrinsic anisotropy of the morphology and the directionality of the charge transport that follows [21].

To bridge this gap here we employ an approach intermediate between the atomistic and the lattice ones, consisting in describing DLC molecules as soft ellipsoids interacting via the Gay-Berne (GB) potential, commonly used in liquid

crystal studies [22]. Because of its computational simplicity, this level of modeling is suitable for simulating devices at the nano and micro scale [23], while taking into account, at least in part, the molecular nature of the system and the temperature dependence of its morphology. The choice of a molecular-level model is important also to try and separate general effects, common to an entire class of compounds [24], and very chemically-specific ones due to the interplay of quantum and structural aspects.

The use of the coarse-grained GB model in combination with charge mobility calculations was introduced by Goto, Takezoe and Ishikawa in [25] for nematics and smectics, and then extended to biaxial-shape particles [26]. Here we slightly modify their method and apply it to the study of charge transport on discotic liquid crystals, focussing on the important family of triphenylene derivatives. To our knowledge, despite a few theoretical studies of their morphology have been published [27–29], atomistic studies of mobility are not available, while numerous experimental observations awaiting a microscopic explanation exist. As far as charge transport in triphenylene DLCs is concerned, a striking experimental observation (Figure 1) is that the mobility increases discontinuously going from the insulating isotropic liquid to the columnar phase and from columnar to crystal. Inside the columnar phase triphenylenes instead show a semiconducting behaviour with a weak increase of mobility on cooling down. A further jump up in mobility is then shown when these materials enter the highly ordered crystalline phase.

Here we aim to see whether our coarse-grained representation of triphenylenes with GB disks, which was shown to reproduce qualitatively the phase diagram of triphenylene DLCs [30], can be also used to predict the main features of their charge mobility dependence on temperature and applied electric field, without having to resort to detailed atomistic simulations and specific QM calculations.

2 Computational Techniques

Molecular level simulations, in which every molecule or monomeric unit is described by a single interacting site, are known as an efficient tool for studying liquid crystals [22,31]. Here we used Monte Carlo (MC) simulations in order to obtain a set of molecular configurations suitable for the subsequent evaluation of the charge mobility. This has been accomplished by means of a in-house Fortran90 code, using the GB potential [32]. This potential has been extensively used in the two last decades to simulate systems of both prolate and oblated ellipsoids [24]. For the discotic particles considered here it was shown in [30,33] that columnar phases are spontaneously formed either by cooling down from the isotropic phase or by heating a columnar crystal. Going into the details of the potential, we recall here its explicit, Lennard-Jones-like expression:

$$U_{ij} = \mathcal{E}\left[\left(\frac{\sigma_{ff}}{r_{ij}-\mathcal{S}+\sigma_{ff}}\right)^{12}-\left(\frac{\sigma_{ff}}{r_{ij}-\mathcal{S}+\sigma_{ff}}\right)^{6}\right], \quad (1)$$

and the parameters describing the interaction and the shape of the discotic molecular model ($\mu = 1$, $\nu = 0$; $\epsilon_{ee} = 9$ and $\epsilon_{ff} = 60$ kcal/mol; $\sigma_{ee} = 19.25$ and $\sigma_{ff} = 3.75$ Å, where ee and ff stand for end-to-end and face-to-face dimer arrangements). These values were derived in reference [30] with a coarse-graining procedure consisting in fitting with the GB energy expression the Lennard-Jones energy calculated from atomistic simulations in columnar phase for a small sample of hexa-thio-octyl triphenylenes.
Actually the GB potential depends only on the ratios of the sigmas and the epsilons through the functions χ and χ':

$$\chi = \frac{(\sigma_{ff}/\sigma_{ee})^2 - 1}{(\sigma_{ff}/\sigma_{ee})^2 + 1}, \quad \chi' = \frac{(\epsilon_{ee}/\epsilon_{ff})^{1/\mu} - 1}{(\epsilon_{ee}/\epsilon_{ff})^{1/\mu} + 1}. \tag{2}$$

With the choice of $\nu = 0$, the interaction function reduces to:

$$\mathcal{E} = 4\,\epsilon_0 \left\{ 1 - \frac{\chi'}{2} \left[\frac{(\hat{\mathbf{r}}_{\mathbf{ij}} \cdot \mathbf{u}_i + \hat{\mathbf{r}}_{\mathbf{ij}} \cdot \mathbf{u}_j)^2}{1 + \chi'(\mathbf{u}_i \cdot \mathbf{u}_j)} + \frac{(\hat{\mathbf{r}}_{\mathbf{ij}} \cdot \mathbf{u}_i - \hat{\mathbf{r}}_{\mathbf{ij}} \cdot \mathbf{u}_j)^2}{1 - \chi'(\mathbf{u}_i \cdot \mathbf{u}_j)} \right] \right\}^{\mu}, \tag{3}$$

where the $\hat{\mathbf{r}}_{\mathbf{ij}}$ is the intermolecular unit vector and $\mathbf{u}_i$, $\mathbf{u}_j$ are the molecular axes. The contact distance function is invaried with respect to the original formulation [32]:

$$\mathcal{S} = \sigma_0 \left\{ 1 - \frac{\chi}{2} \left[\frac{(\hat{\mathbf{r}}_{ij} \cdot \mathbf{u}_i + \hat{\mathbf{r}}_{ij} \cdot \mathbf{u}_j)^2}{1 + \chi(\mathbf{u}_i \cdot \mathbf{u}_j)} + \frac{(\hat{\mathbf{r}}_{ij} \cdot \mathbf{u}_i - \hat{\mathbf{r}}_{ij} \cdot \mathbf{u}_j)^2}{1 - \chi(\mathbf{u}_i \cdot \mathbf{u}_j)} \right] \right\}^{-\frac{1}{2}}. \tag{4}$$

The two parameters ϵ_0 and σ_0 serve to scale the simulation energy and distance units [34]. The translation between simulations and real units is given in the next section on the basis of the simulation results.

As far as the calculation of mobilities at room temperature is concerned, these columnar systems are strongly unidimensional and the charge hopping occurs between first neighbours in the same column. In the GB potential this distance is determined by the parameter σ_{ff}. As a consequence the intercolumnar distance, which instead depends on the value of σ_{ee}, is not very relevant as the intercolumnar charge hopping is very unlikely. This confers more generality to our model, which can be extended to any discotic aromatic core substituted by non-polar chains. To increase its realism, the value of σ_{ee} can be tuned as to obtain the desired intercolumnar distance (e.g. 19–25 Å in triphenylenes [35]).

We ran simulations in the NPT ensemble for a N=4000 particle cell at a fixed pressure P=2 $\epsilon_0/{\sigma_0}^3$, and increased the simulation temperature k_BT in a sequence of runs from the initial value of 0.2 ϵ_0 to 0.55 ϵ_0. At first we created an oriented crystal sample with the help of a potential aligning along the cartesian axis Z ($U_i^F = -k(\vec{Z} \cdot \mathbf{u}_i)^2$ with $k = 3\epsilon_0$), then we switched off this potential and heated and equilibrated the sample in the aforementioned range of temperatures, adopting 3D periodic boundary conditions. The box shape was on purpose chosen to be more elongated along the Z direction, i.e. parallel to the column axes, in order to achieve a better phase sampling in the direction of the

applied electric field during the calculations of mobility. After equilibration a production run was performed for 1.5 to 3.0 millions of MC cycles depending on the temperature.

For each temperature, we then extracted 150 configurations and used the molecular coordinates to perform charge transport simulations and obtain the mobility profiles through the crystal, columnar liquid crystal and isotropic phases, as a function of various parameters. The charge transport rate constants ν_{ij} between active sites were calculated via the Miller-Abrahams hopping rate, based originally on the assumption of a vibrational-assisted tunneling mechanism [36]:

$$\nu_{ij} = a_0\ J^2(r_{ij}) \begin{cases} \exp[-\Delta G/(k_B T)] & \text{if } \Delta G > 0 \\ 1 & \text{if } \Delta G < 0 \end{cases} \tag{5}$$

$$\text{with} \quad \Delta G = U_j - U_i - q\vec{E} \cdot \vec{r}_{ij} \tag{6}$$

$$\text{and} \quad J(r_{ij}) = J_0 \exp\left(-\Gamma_{ij} r_{ij}\right), \tag{7}$$

where $\vec{r}_{ij}$ is the distance vector between the centers of mass of molecules (sites) i and j, $q\vec{E} \cdot \vec{r}_{ij}$ is the work required for moving a charge q of $\vec{r}_{ij}$ in an electric field $\vec{E}$ parallel to the column axes. U_i and U_j are the energies of the carriers at sites i, j, J is the transfer integral, J_0 is the transfer integral at $r_{ij} = 0$, Γ_{ij} is the inverse decay length and a_0 is a constant prefactor (here set to $1{\times}10^{10}$ s^{-1} eV^{-2} in order to have mobilities in the range of the experimental values).

The values of the site energies U_i were extracted from a gaussian distribution of width θ. Here we have used both the arbitrarily chosen values $\theta = 0, 2, 3\ k_B T$ and temperature-dependent standard deviations calculated during the MC simulation. The positional disorder [4](i. e. the variation of the transfer integral with the fluctuation of molecular positions) was instead included directly, like in [25] and in atomistic studies, through the use of simulated configurations for the calculation of the instantaneous intermolecular distances r_{ij} in Equation 7. This approach has on one hand the advantage of calculating the structural disorder, normally not accessible in QM studies [37], rather than using it as an empirical parameter to fit experimental data [15, 38–40]. On the other hand the method retains the simplicity of Miller-Abrahams expression for the square of transfer integral, instead of resorting to more complicated and accurate schemes [11,21,26,37], that in this case are not justified, given the coarse-grained modeling of molecules.

It should also be noted that an additional source of energetic disorder, deriving from the rotational motion of molecules about the columnar axis [3,11,28,41], is present in real discotic materials. This effect is neglected here due to the $D_{\infty h}$ symmetry of the GB model, which does not allow to define a twist angle - all angles are actually isoenergetic.

It is important to point out that our approach is different from the Gaussian Disorder Model (GDM) that has been extensively used in the last two decades for simulating and interpreting experimental mobility measurements for disordered organic materials [15,38,42], as here the transfer integrals are calculated as

a function of the molecular positions. The GDM neglects the spatial correlation between the sites [43] and consists in extracting randomly both the site energies U_i and the transfer integrals J from gaussian distributions of given width, assuming that their average values do not change with temperature. The method is appealing as it allows predicting mobilities with analytical equations [44] once the extent of the positional and energetic disorder is known, or alternatively to extract the standard deviations of the two sources of disorder by fitting experimental mobility trends. We will show in the discussion that while this model could be appropriate for describing DLCs at a given temperature or in a given phase, it is not applicable in the full temperature range explored in this study. In the Miller-Abrahams equation, the transfer integral between two sites is assumed to decay exponentially with characteristic length Γ_{ij}^{-1} (Equation 7), with its squared value appearing in the transfer rate (Equation 5). In our simulations, we used four different parameterizations for the transfer integrals. Three were obtained by fitting the value of the transfer integral at $r = 0$ (J_0^2) and its inverse decay length (Γ_{ij}) to the radial dependence of the hole transfer integral for three differently substituted triphenylenes, as calculated *ab initio* by Siebbeles and coworkers [45]. We label these parameterizations as H, OCH_3 and SCH_3 as they correspond to calculations for cofacial triphenylene dimers with six H, OCH_3 and SCH_3 groups attached in the 2, 3, 6, 7, 10, and 11 positions, respectively. The fitting parameters are reported in Table 1, while the corresponding profiles are plotted in Figure 2 as well as the values calculated in ref. [45], which are well fitted by Equation 7. We also evaluated the effect of an arbitrary parameterization introduced to assess the effect of a longer decay length of the transfer integral with respect to typical values for triphenylenes. We called this set of parameters "long range" (LR) and we employed for it $\Gamma_{ij} = 0.5$ Å^{-1} and $J_0 = 1$ eV. All four parameterizations were applied to the evaluation of the transfer integral for the same set of simulated trajectories, i. e. we took advantage of the possibility offered by simulations to check the effect of chemical differences in the idealized case that the structure of the system is left unchanged.

Also in the case of the transfer integral, we neglect its dependence on the twist angle between two neighbouring molecules [3, 5, 37, 41, 45], and we treat the values in Figure 2 as effective, rotationally averaged quantities.
The charge occupation of the sites of each configuration was evaluated by solving the Master Equation (ME), hence assuming that transport takes place via a Markov process with time-independent hopping transition rate ν_{ij} of the charge (hole) from site i to j. In this case it is possible to use a linearized ME which is valid in the limit of low charge carrier concentration [16, 46]:

$$\frac{dP_i}{dt} = \sum_{i \neq j} [\nu_{ji} P_i - \nu_{ij} P_j] = 0 \qquad (8)$$

where the P_i are the probabilities of finding a charge on a given site. Once the charge occupations for each configuration were known, and once fixed the total

charge $\sum_i P_i$ to 1, we calculated the mobility μ for each snapshot as [16]:

$$\mu = \frac{\sum_i P_i \sum_j \nu_{ij}(\vec{r}_{ij} \cdot \vec{E})}{|E^2|} \tag{9}$$

The final value of the mobility is then evaluated as the arithmetic mean over the configurations. A sufficiently large number of configurations is necessary as the single values of the mobility are very scattered: this effect is related to the necessity of averaging not only over the fluctuations of molecular positions but also over the effect of the fixed energetic and positional disorder. In our case the convergence of mobility was reached after approximately 50 configurations.

3 Results and discussion

The MC simulations for a system of N=4000 disks confirm the heating phase diagram sketched in [30] for a smaller system composed of N=1000 molecules: at P=2 $\epsilon_0/{\sigma_0}^3$, upon heating, the system exhibits three phases: a rectangular crystal (K), a hexagonal columnar liquid crystal (C) and an isotropic liquid (I); this phase sequence corresponds to the most common one reported for real DLC semiconductors, such as triphenylenes and hexabenzocoronenes [47]. From the snapshots shown in Figure 3 it appears clear that with increasing temperature the phase changes are accompanied by an increase of orientational and translational disorder which ends, in the isotropic phase, with the destruction of the 1D positional order. We note that a nematic discotic is not observed in the simulations, in agreement with real systems. The internal energy (U/N) and number density (N/V) profiles, also reported in Figure 3, allow to identify, in correspondence with sharp discontinuities, the phase transition temperatures (indicated with vertical dotted lines in the figures). It is also worth noting that, with respect to real and flexible molecules, the density variations with temperature are overestimated, and that this known limitation of rigid molecular models may affect also the temperature dependence of the mobility, e. g. through modulation of intermolecular distances.

The variations of positional order are evidenced at best by the radial distributions of molecular centers of mass g(r), plotted in Figure 4. In the K and C phases, sharp peaks are present at $\simeq$0.4, 0.8, 1.2 σ_0, corresponding to the first, second and third neighbour molecule along the column axes, respectively. The main differences between the K and C phases are reflected in a general broadening of the peaks in the latter, and in the peak at $\simeq$1.9 σ_0, representing the intercolumnar distance, which is featureless in the C phase and splits in the K due to the onset of a rectangular packing [3, 30]. In the isotropic phase the radial distribution becomes almost uniform except at short range, where the tendency of disk-shaped molecules to stack in parallel dimers is witnessed by the persistence of the peak at 0.4-0.5 σ_0. The important variations of g(r) in the different phases, in particular at short range, where the transfer integral is not negligible, should produce remarkable differences in the charge mobility from one phase to another.

On the basis of these observables, it is now possible to establish a relation between GB model units and real ones. Regarding the length scales, matching the position of the simulated first neighbour peak of the g(r) (0.4 σ_0) with the typical intermolecular distance in crystal phase (3.5-3.7 Å [13, 48]) gives a simulation-to-real scaling σ_0 of roughly 9 Å. For the temperature, assuming a C→I transition temperature of 400 K (cf Figure 1) and taking 0.5 ϵ_0 as the simulated one, gives a scaling factor of about 800 K for temperatures, which tranlates in roughly 0.07 eV for energies. We then refer to these approximate real units in the remainder of the article, as they were used in the calculations of all the observables relying on Equation 5.

Focusing on the assessment of the mobility for our discotic systems, we compare, among the several techniques employed in the last two decades [49–55], with pulse-radiolysis time-resolved microwave conductivity (PR-TRMC) measurements. This technique in fact provides "local", bulk phase mobility values not dependent on the grain boundaries and their concentration, and it is less sensitive to experimental parameters and setups with respect to other techniques [4]. As mentioned earlier on, the measurements, performed mainly by Warman and coworkers, demonstrated that for triphenylenes the phase transition from the K to the C phase is accompanied by a sudden drop of the mobility [53] (Figure 1) of up to an order of magnitude, attributed to the increased positional disorder, while in the two phases the temperature dependence is surprisingly rather weak. The mobility drops to zero or to very low values in the isotropic phase, where the material becomes essentially an insulator, and its value is often not even reported in experimental studies.

Before proceeding to the evaluation of the mobility from the simulations, it is interesting to monitor the most important parameter for charge transport, i. e. the ensemble-averaged square transfer integral $\langle J^2 \rangle$, calculated with Equation 7 between the nearest neighbours (see Figure 4) and plotted against temperature in Figure 5 for the SCH_3 parameterization (all the other cases show qualitatively similar trends). First of all we note, comparing Figure 5 with Figure 2, that, consistently with atomistic studies [3], thermal fluctuations determine average values which are much lower than it could naïvely be expected from the optimal situation of a cofacial dimer at a separation of 3.5 Å, with the effect being particularly relevant for the C phase. Indeed the sequence of phases and the ensuing structural change have a strong impact on $\langle J^2 \rangle$, with sudden changes at the phase transitions which are reminiscent of the drops in experimental mobilities (Figure 1), but also are affected by the change of density of the system (Figure 3). On the contrary, the standard deviations do not show a marked temperature dependence, probably because the increase of positional disorder corresponds to distributions of the square transfer integral more and more shifted towards zero and hence narrower, as shown by the selected examples in the inset of Figure 5. In support to our results we observe that the values obtained here for the mean square transfer integral (0.01-0.001 eV^2) and for its standard deviation (0.002-0.003 eV^2) are consistent with QM calculations performed on atomistic molecular dynamics simulations trajectories of hexaben-

zocoronene [2], phthalocyanine [3] and perylene derivatives [11].

Another important parameter in determining the final value of mobility is the diagonal or energetic disorder, consisting in the fluctuations of the site (orbital) energies of the molecules due to thermal motion and intermolecular interactions. We estimated these fluctuations by calculating, for each molecule i, the total intermolecular energy $U_i = \sum_{j \neq i}^{N} U_{ij}$, its average distribution during the MC simulation, and its standard deviation θ [56]. The distributions, shown in Figure 6a, become broader at increasing temperature, and shifted towards more positive energies as expected; besides, in the K and C phases, they visibly deviate from the standard gaussian shape, which is instead recovered in the isotropic samples. The standard deviation of the distributions θ grows linearly with temperature in the K, C, and I phases, exhibiting steps only at the phase transition, while $\theta/(k_B T)$ is instead fairly constant with temperature, with a weak counterintuitive tendency to decrease in any phase, maintaining however the sudden small steps at the phase transitions shown by θ (Figure 6b). Again the calculated values are of the same order of magnitude of the values reported in the literature by more detailed studies [2, 11]; besides, the drop of $\theta/(k_B T)$ going from the K to the C phase has been reported also for n-dodecyl substituted hexabenzocoronenes by Andrienko and collaborators [2].

The extent of energetic disorder and the depth of the traps $U_j - U_i$ are fundamental in determining the electric field dependence of the mobility, and consequently in the choice of the value of E to be used in Equation 5. For that purpose, we plot in Figure 7 the mobility values calculated for a range of fields and temperatures corresponding to K and C phases, with the diagonal disorder extracted randomly from gaussian distribution with width $\theta/(k_B T)$, as plotted in Figure 6b. From the straight lines in the log-log plot it emerges that in the range of fields we used, close to typical experimental values, the logarithm of the mobility of the material roughly changes with the square root of the electric field, and that in this case electric fields up to 1×10^6 V/cm have a limited influence over the temperature dependence of the mobilities. We chose a value of $E = 0.3 \times 10^6$ V/cm in the mobility calculations, corresponding then to a regime of field-assisted detrapping with the depth of the traps of the same order of magnitude of the thermal energy (Poole-Frenkel like behavior).
In Figure 8 we show the simulated trend of mobilities, to be compared with the experimental ones in Figure 1. All the main experimental features are indeed well reproduced: $\mu(T)$ is clearly non-Arrhenius and nearly constant in K phase, with sharp decreases associated both with the K→C and the C→I phase transitions, and drops to very small (zero) values in the isotropic phase [57]. On the negative side, the slow decay of mobility in C phase reported for most triphenylene compounds is overemphasized here; as already discussed, we attribute this deficiency to the unrealistic density changes in the C phase obtained for this rigid molecular model.

With regard to the dependence of mobility on diagonal disorder, the simulations predict a rather low value for the latter ($\theta/(k_BT)$ lower than 2, or θ <50 meV if we refer to absolute units, Figure 6), but we calculated mobilities also for $\theta/(k_BT)$=0, 2, 3, as shown in Figure 8. Surprisingly enough, the variation of $\theta/(k_BT)$ in practice scales the absolute value of the mobility, but does not affect the shape of the μ vs T curve; once again this behaviour is in agreement with the results in reference [2]. In particular, the temperature-independence in the K phase is retained for all $\theta/(k_BT)$ values, indicating that the driving force for this trend and the deviations from the predictions of the GDM evidenced in reference [42] must be found in the morphology-related temperature dependence of $\langle J^2 \rangle$.

Finally, in Figure 9 we analyze the effect of possible chemical substitution at the tryphenylene core on mobility profiles (Table 1). The changes are very similar to the ones induced by the diagonal disorder, even if in this case we are varying the values of $\langle J^2 \rangle$ and of its standard deviation, suggesting the difficulties of disentangling the two effects by fitting experimental data [16, 42] with the GDM equations. Besides, at least in the K phase, the temperature independence is again retained by all parameter sets, a further confirmation that the well ordered columns of the K phase do not change their structure in this temperature range. Another aspect that emerges from varying the radial parameters is the paramount importance of even small chemical changes to the aromatic core, which may easily determine a variation of one or two order of magnitude of mobility, even in the limiting case that they do not alter the structure of the system, like assumed here. It is also worth noting how the temperature dependence of mobility, in particular in the less ordered C and in the disorderer I phase, can be weakened by increasing the spatial range of the off-diagonal interactions. In other words, it strongly depends on the value of the inverse decay length of the transfer integral Γ_{ij} in Equation 5: smaller values of Γ_{ij}, like the ones used here for the LR and even the H parameterizations, produce in fact weaker decreases of μ at increasing temperature with respect to the OCH_3 and SCH_3 cases. Finally, we notice that the two latter sets yields to very similar mobility values, as seen in experiments (Figure 1).

4 Conclusions

In this work, we employed molecular level Monte Carlo simulations to reproduce qualitatively the phase diagram and morphology of triphenylenes discotic liquid crystals and evaluate their charge carrier mobility. Transfer rates were calculated with the Miller-Abrahams approximation, with transfer integrals parametrized on quantum chemistry values and evaluated directy from the simulated structures. Also the extent of energetic disorder was calculated from the Gay-Berne intermolecular energies and introduced into the Miller-Abrahms rate as a random gaussian disorder.
We estimated the energetic disorder to be rather small, of the order of 0.05 eV,

while the fluctuations of the transfer integral are predicted to be around 0.003 eV^2. Both values are in agreement with the results of more specific studies for discotic liquid crystals [2, 3, 11].

We found a weak, Poole-Frenkel like dependence of mobility on the electric field, while diagonal and off-diagonal disorders have similar, important effects, which however scale only the absolute mobility values, barely changing its temperature dependence, contrary to what normally happens in disordered amorphous materials or in systems with strong dipolar disorder. [15, 38, 42]. Here this dependence in fact is dominated by the variation with temperature of the average value of the squared transfer integral, which is constant in the crystal phase and slowly decreasing in the columnar phase. These variations of the transfer integrals are at the origin of the failure of the gaussian disorder model for triphenylenes substituted with apolar chains (hence, with no sources of dipolar energetic disorder) [42], despite the approximation of a gaussian shape for site energy and transfer integral distributions seems to be valid.

On the computational side, we showed that a simple model is able to reproduce essentially from first principles the typical behaviour of experimental triphenylene mobilities with temperature. We believe that this methodology has possible applications in the simulations of organic electronics devices.

Acknowledgements

We thank Dr. Yoann Olivier (University of Mons) for several helpful conversations on charge transport modeling and discotic semiconductors.
The research leading to these results has received funding from the European Community's Seventh Framework Programme (FP7/2007-2013) under grant agreement n.° 212311 of the ONE-P project.
We dedicate this article to the memory of our gentle and smart colleague Manuele Lamarra, who most sadly left us in March 2011.

References

1. B. Walker, C. Kim, and T.-Q. Nguyen, *Chem. Mater.*, 2011, **23**, 470–482.
2. J. Kirkpatrick, V. Marcon, K. Kremer, J. Nelson, and D. Andrienko, *J. Chem. Phys.*, 2008, **129**, 094506.
3. Y. Olivier, L. Muccioli, V. Lemaur, Y. H. Geerts, C. Zannoni, and J. Cornil, *J. Phys. Chem. B*, 2009, **113**, 14102–14111.
4. V. Coropceanu, J. Cornil, D. A. da Silva Filho, Y. Olivier, R. Silbey, and J.-L. Brédas, *Chem. Rev.*, 2007, **107**, 926–952.
5. V. Lemaur, D. A. da Silva Filho, V. Coropceanu, M. Lehmann, Y. Geerts, J. Piris, M. G. Debije, A. M. van de Craats, K. Senthilkumar, L. D. A. Siebbeles, J. M. Warman, J.-L. Brédas, and J. Cornil, *J. Am. Chem. Soc.*, 2004, **126**, 3271–3279.
6. A. Calò, P. Stoliar, M. Cavallini, S. Sergeyev, Y. H. Geerts, and F. Biscarini, *J. Am. Chem. Soc.*, 2008, **130**, 11953–11958.

7. E. Pouzet, V. De Cupere, C. Heintz, J. W. Andreasen, D. W. Breiby, M. M. Nielsen, P. Viville, R. Lazzaroni, G. Gbabode, and Y. H. Geerts, *J. Phys. Chem. C*, 2009, **113**, 14398–14406.
8. A. Calò, P. Stoliar, M. Cavallini, Y. H. Geerts, and F. Biscarini, *Org. Electron.*, 11, **12**, 851–856.
9. B. R. Kaafarani, *Chem. Mater.*, 2011, **23**, 378–396.
10. F. Xinliang, V. Marcon, W. Pisula, M. R. Hansen, J. Kirkpatrick, F. Grozema, D. Andrienko, K. Kremer, and K. Müllen, *Nat. Mater.*, 2009, **8**, 421–426.
11. J. Idé, R. Méreau, L. Ducasse, F. Castet, Y. Olivier, N. Martinelli, J. Cornil, and D. Beljonne, *J. Phys. Chem. B*, 2011, **115**, 5593–5603.
12. F. May, V. Marcon, M. R. Hansen, F. Grozema, and D. Andrienko, *J. Mater. Chem.*, 2011, **21**, 9538–9545.
13. F. C. Grozema and L. D. A. Siebbeles, *Int. Rev. Phys. Chem.*, 2008, **27**, 87–138.
14. D. L. Cheung and A. Troisi, *Phys. Chem. Chem. Phys.*, 2008, **10**, 5941–5952.
15. P. M. Borsemberger, L. Pautmeier, and H. Baessler, *J. Chem. Phys.*, 1991, **94**, 5447–5454.
16. W. F. Pasveer, J. Cottaar, C. Tanase, R. Coehoorn, P. A. Bobbert, P. W. M. Blom, D. M. de Leeuw, and M. A. J. Michels, *Phys. Rev. Lett.*, 2005, **94**, 206601.
17. L. Y. Meng, Y. Shang, Q. K. Li, Y. F. Li, X. W. Zhan, Z. G. Shuai, R. G. E. Kimber, and A. B. Walker, *J. Phys. Chem. B*, 2010, **114**, 36–41.
18. H. Yan, S. Swaraj, C. Wang, I. Hwang, N. C. Greenham, C. Groves, H. Ade, and C. R. McNeill, *Adv. Mater.*, 2010, **20**, 4329–4337.
19. M. Gruber, B. A. Stickler, G. Trimmel, F. Schürrer, and K. Zojer, *Org. Electron.*, 2010, **11**, 1999–2011.
20. J. J. M. van der Holst, F. W. A. van Oost, R. Coehoorn, and P. A. Bobbert, *Phys. Rev. B*, 2011, **83**, 085206.
21. J. C. Sancho-García, A. J. Pérez-Jiménez, Y. Olivier, and J. Cornil, *Chem. Phys. Phys. Chem.*, 2010, **12**, 9381–9388.
22. R. Berardi, L. Muccioli, S. Orlandi, M. Ricci, and C. Zannoni, *J. Phys.:Condens. Matter*, 2008, **20**, 463101.
23. M. Ricci, M. Mazzeo, R. Berardi, P. Pasini, and C. Zannoni, *Faraday Discuss.*, 2010, **144**, 171–185.
24. C. Zannoni, *J. Mater. Chem.*, 2001, **11**, 2637–2646.
25. M. Goto, H. Takezoe, and K. Ishikawa, *Phys. Rev. E*, 2007, **76**, 040701.
26. M. Goto, H. Takezoe, and K. Ishikawa, *J. Chem. Phys.*, 2010, **132**, 054506.
27. G. Cinacchi, R. Colle, and A. Tani, *J. Phys. Chem. B*, 2004, **108**, 7969–7977.
28. L. Muccioli, R. Berardi, S. Orlandi, M. Ricci, and C. Zannoni, *Theor. Chem. Acc.*, 2007, **117**, 1085–1092.
29. L. A. Haverkate, M. Zbiri, M. R. Johnson, B. Deme, F. M. Mulder, and G. J. Kearley, *J. Phys. Chem. B*, 2011, **115**, 13809–138161.
30. S. Orlandi, L. Muccioli, M. Ricci, R. Berardi, and C. Zannoni, *Chem. Centr. J.*, 2007, **1**, 15.

31. M. R. Wilson, *Chem. Soc. Rev.*, 2007, **36**, 1881–1888.
32. J. G. Gay and B. J. Berne, *J. Chem. Phys.*, 1981, **74**, 3316–3319.
33. I. Miglioli, L. Muccioli, S. Orlandi, M. Ricci, R. Berardi, and C. Zannoni, *Theor. Chem. Acc.*, 2007, **118**, 203–210.
34. *For consistency with reference [30], we used in the Monte Carlo simulations the arbitrary factors* $\epsilon_0 = 0.3$ *and* $\sigma_0 = 1.925$. *Note that these units were used but erroneously non reported in [30].*
35. A. M. van de Craats *Charge Transport in Self-Assembling Discotic Liquid Crystalline Materials* PhD thesis, Delft University of Technology, 2000.
36. A. Miller and E. Abrahams, *Phys. Rev.*, 1960, **120**, 745–755.
37. M. M. Mikolajczyk, P. Toman, and W. Bartkowiak, *Chem. Phys. Lett.*, 2010, **485**, 253–257.
38. H. Baessler, *Phys. Stat. Sol. B 175*, 1993, **175**, 15–55.
39. R. H. Young, *J. Chem. Phys.*, 1995, **103**, 6749–6767.
40. L. B. Schein and A. Tyutnev, *J. Phys. Chem. C*, 2008, **112**, 7295–7308.
41. M. A. Palenberg, R. J. Silbey, M. Malagoli, and J.-L. Brédas, *J. Chem. Phys.*, 2000, **112**, 1541–1546.
42. A. Ochse, A. Kettner, J. Kopitzke, J. H. Wendor, and H. Bässler, *Phys. Chem. Chem. Phys.*, 1999, **1**, 1757–1760.
43. S. V. Novikov, D. H. Dunlap, V. M. Kenkre, P. E. Parris, and A. V. Vannikov, *Phys. Rev. Lett.*, 1998, **81**, 4472–4475.
44. N. Tessler, Y. Preezant, N. Rappaport, and Y. Roichman, *Adv. Mater.*, 2009, **21**, 2741–2761.
45. K. Senthilkumar, F. C. Grozema, F. M. Bickelhaupt, and L. D. A. Siebbeles, *J. Chem. Phys.*, 2003, **119**, 9809–9817.
46. N. Rappaport, Y. Preezant, and N. Tessler, *Phys. Rev. B*, 2007, **76**, 235323.
47. S. Sergeyev, W. Pisula, and Y. H. Geerts, *Chem. Soc. Rev.*, 2007, **36**, 1902–1929.
48. E. Fontes, P. A. Heiney, and W. H. de Jeu, *Phys. Rev. Lett.*, 1988, **61**, 1202–1205.
49. D. Adam, F. Closs, T. Frey, D. Funhoff, D. Haarer, H. Ringsdorf, P. Schuhmacher, and K. Siemensmeyer, *Phys. Rev. Lett.*, 1993, **70**, 457–460.
50. N. Boden, R. J. Bushby, J. Clements, B. Movaghar, K. J. Donovan, and T. Kreouzis, *Phys. Rev. B*, 1995, **52**, 13274–13280.
51. T. Kreouzis, K. J. Donovan, N. Boden, R. J. Bushby, O. R. Lozman, and Q. Liu, *J. Chem. Phys.*, 2001, **114**, 1797–1802.
52. J. M. Warman and A. M. van de Craats, *Mol. Cryst. Liq. Cryst.*, 2003, **396**, 41–72.
53. J. M. Warman, M. P. de Haas, G. Dicker, F. C. Grozema, J. Piris, and M. G. Debije, *Chem. Mater.*, 2004, **16**, 4600–4609.
54. M. P. Debije, J. Piris, M. P. de Haas, J. M. Warman, Z. Tomovic, C. D. Simpson, M. D. Watson, and K. Mullen, *J. Am. Chem. Soc.*, 2004, **126**, 4641–4645.
55. J. Piris, M. G. Debije, N. Stutzmann, B. W. Laursen, W. Pisula, M. D. Watson, T. Bjørnholm, K. Müllen, and J. M. Warman, *Adv. Funct. Mater.*, 2004, **14**, 1053–1061.

56. *Differently from the most common choice in the literature, we use here the symbols U for the site energies and θ for their standard deviation, so to avoid confusion with the Gay-Berne parameters ϵ and σ.*

57. P. G. Schouten, J. M. Warman, M. P. de Haas, M. A. Fox, and H.-L. Pan, *Nature*, 1991, **353**, 736–737.

58. A. M. van der Craats, J. M. Warman, M. P. de Haas, D. Adam, J. Simmerer, D. Haarer, and P. Schuhmacher, *Adv. Mater.*, 1996, **8**, 823–826.

Table 1: Parameterization of the distance dependence of hole transfer integrals to be used in eq.5, fitted to the values calculated in ref. [45] for hexa- H, OCH_3 and SCH_3-substituted triphenylenes. LR is a long range parameterization also studied in this work.

	H	OCH_3	SCH_3	LR
J_0 (eV)	5.74	34.4	16.3	1.0
Γ_{ij} (Å^{-1})	1.12	1.61	1.24	0.5

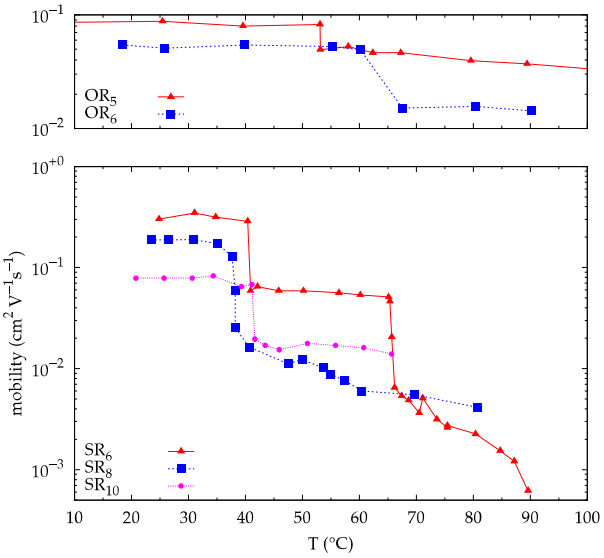

Figure 1: Temperature dependence of charge carrier mobility of hexasubstituted triphenylene discotic semiconductors in crystal and columnar phases as obtained in pulse-radiolysis time-resolved microwave conductivity studies (R_n= linear alkyl chains of n carbons, data extracted from references [35, 52, 58]). Except for SR_6, which present an intermediate columnar helical phase [48], the values at low T are measured in crystal phase and the values at high T in the columnar hexagonal phase.

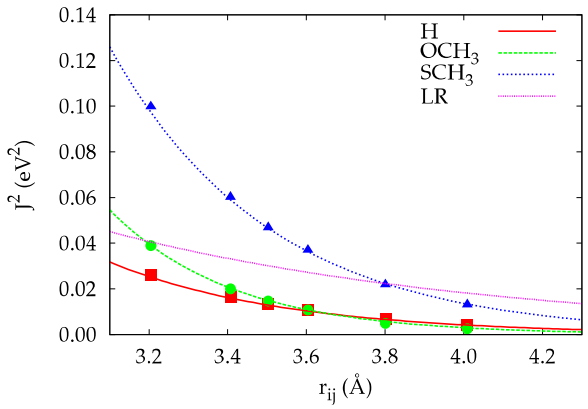

Figure 2: A plot of the square of the hole transfer integral calculated at DFT/triple-ζ level for model triphenylene dimers, extracted from ref. [45] (red squares: unsubstituted, green circles: hexa -OCH_3 substituted, blue triangles: hexa -SCH_3 substituted) and of their interpolation curves with Equation 7 (parameters are reported in Table 1). The curve obtained for a the long interaction range parameterization (LR) used in this work is also shown.

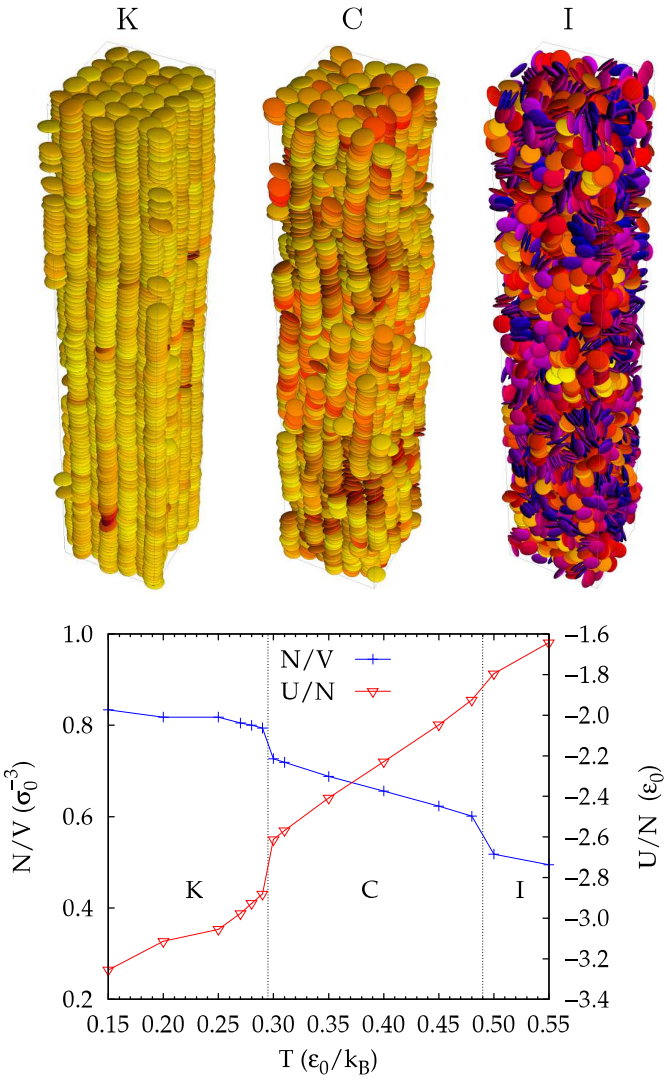

Figure 3: Top: snapshots of the 4000 molecules sample at three different temperatures, corresponding to crystal (K), liquid-crystalline columnar (C) and isotropic liquid phases (I). Bottom: internal energy (U/N) and number density (N/V) profiles (simulation units). Vertical lines indicate the phase transition temperatures.

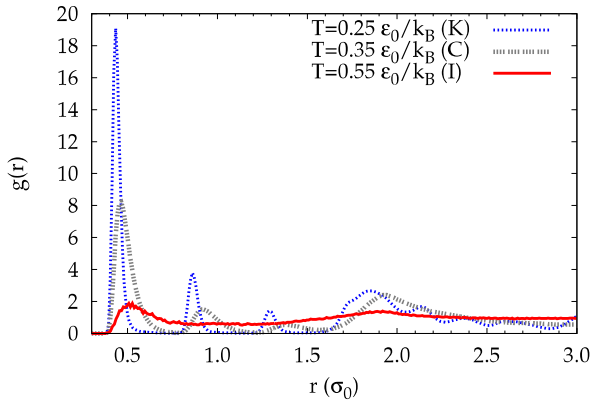

Figure 4: Radial distribution functions obtained by Monte Carlo simulations for the K, C and I phase. The vertical line indicates the cutoff chosen for the individuation of the first neighbours and the calculation of the transfer integral distributions.

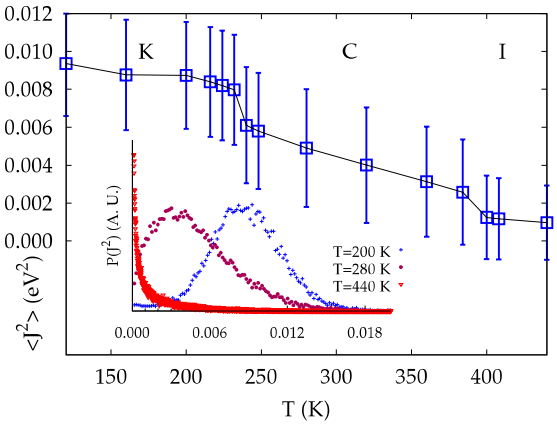

Figure 5: Ensemble-averaged squared transfer integral, evaluated as the radial part of the Miller-Abrahams formula for the nearest neighbour transfer rate as a function of temperature, calculated for the SCH_3-substituent parameterization. In the inset: distribution of the squared transfer integral in the K, C, and I phases.

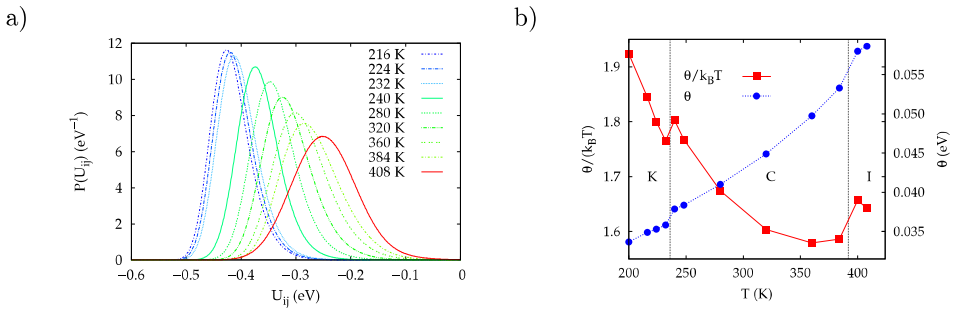

Figure 6: Left: distributions of the site energies calculated with MC simulations. Right: average values of site energies standard deviations θ (blue) and $\theta/(k_BT)$ (red) evaluated from simulations. Vertical lines indicate the phase transition temperatures.

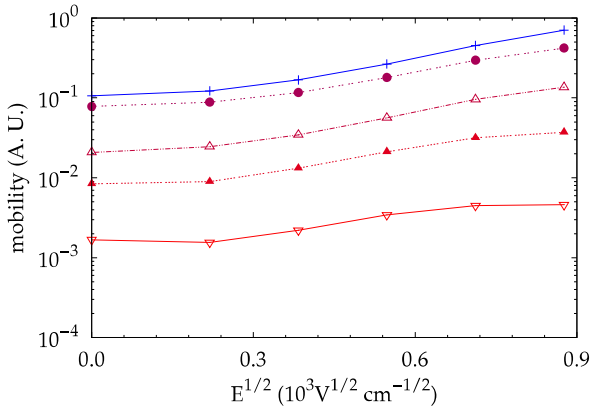

Figure 7: Effect of the electric field on the mobility profiles, evaluated at different temperatures for the SCH_3-substituent parameterization and with MC diagonal disorder.

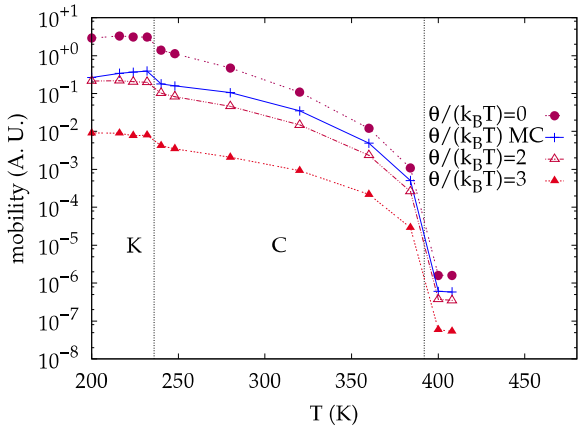

Figure 8: The mobility (arbitrary units) profiles evaluated for different degrees of diagonal disorder as a function of the reduced temperature for the SCH_3-substituent parameterization.

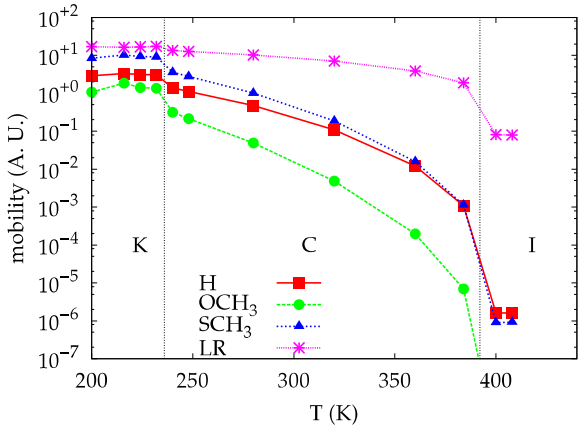

Figure 9: Mobility profiles of model triphenylenes calculated with $\theta/(k_BT) = 0$ as a function of the reduced temperature and for different chemical parameterizations of the square transfer integral.